Kochi Chapter

Indian Geotechnical Conference
IGC 2022
15th – 17th December, 2022, Kochi

Rock mass characterisation and delineation of weak zones in a foundation regime using integrated geophysical methods: a case study from Mangalore, India

S. Nelliat[1], P. C. Jha[1], B. Butchi Babu[1], K. Goverdhan[1], Y. V. Sivaram[1], V. Shashi Nath[1] and Jiby Francis[2]

[1] National Institute of Rock Mechanics, Bengaluru - 560070
[2] Ex-Project Fellow, NIRM, Bengaluru
sandeepnelliat@gmail.com

Abstract. A refinery complex has been operational since 1988 in north Mangalore which is a part of the Western Ghats. The processing units and pipe racks were installed over the benches developed between the elevation of RL=12 m to RL=65 m. During the incessant rains in August 2019, ground destabilization, minor landslides, slope failures and heavy water discharge were observed within the refinery campus. One such landslide damaged the foundation area of a major piperack leading to disruption in some refinery operations. To plan the rock reinforcement and foundation restoration works, it was extremely important to assess the subsurface rock mass condition and to delineate the damage zone, water saturated areas and destabilised zones. A comprehensive geophysical investigation was taken up using multiple methods to accurately assess the subsurface ground condition and to estimate the in-situ rock mass properties.

Four different methods vis-á-vis, crosshole seismic tomography, electrical resistivity imaging, seismic refraction survey and MASW survey was used to investigate and accurately deciphering the strata condition, delineating the groundwater flow path and derive the Poisson's ratio in-situ. Results of the integrated study helped in understanding the characteristics of the lateritic formations and its behaviour under saturated conditions. It showed that changes to the topography had modified the subsurface drainage pattern. The seismic velocity ratio $(\frac{Vp}{Vs})$ in the overburden showed, how it is related to soil condition when it changes from dry to wet and finally water saturated. The Poisson's ratio of lateritic soil in some of the study area was seen to be $\nu = 0.44 - 0.48$, indicating the extent in loss of rigidity leading to failure.

Keywords: Crosshole seismic tomography, electrical resistivity imaging, seismic refraction survey, MASW, lateritic soil, weak rock mass, slope failure, piperack foundation, Poisson's ratio.

1 Introduction

A refinery complex was setup near Mangalore by hill-site development involving levelling of hillocks and filling of minor valleys in the hilly tracts (granitic gneiss

with a thick laterite cap) of the Western Ghats. Various refinery structures including tankages, distillation units, recovery facilities and piperacks were installed over the wide benches developed between elevation of RL=12-65 m. Being a part of the tropical monsoon system, the Western Ghats receive more than 2700 mm of annual rainfall and hence the rocks are characterized by laterization and deeper level weathering. It is expected that large scale modification of topography in the refinery complex would have adversely affect the subsurface drainage pattern. An interaction with the site engineers, brought out that the foundation design for existing plant and facilities was done based on geotechnical investigations and drilling data. Such investigations provide point information and do not reveal the actual profile of weathered layer or the hard rock.

In August 2019, the area around Mangalore received incessant rains. Several instances of ground destabilization involving minor landslides, slope failures, ground heaving and sinkhole formation was reported from within the refinery campus. One such land slide happened at the foundation area of a piperack adjacent to the DHDT Unit and as a result the refinery operations had to be partial stopped. To accomplish comprehensive ground restoration and strata reinforcement, it was necessary to scientifically assess the rock mass condition and mapping of the subsurface flow path of groundwater. Geophysical investigations were carried out from surface and boreholes using four methods vis-á-vis, Seismic Refraction Survey (SRS), Electrical Resistivity Imaging (ERI), Multichannel Analysis of Surface Waves (MASW) and Cross-borehole Seismic Tomography (CST). The P-wave & S-wave velocities and electrical resistivity distribution in the subsurface was used to characterise the ground in terms of its strength parameters and hydrogeological condition respectively. The overall assessment of the strata condition was made by drawing inferences from the 2D geophysical sections and integrating it with the observed site conditions and the topography. The results of study helped the engineers in formulating a restoration plan for the failed structure and in laying a proper drainage system within the refinery campus.

2 Geology of the study area

The Western Ghats are a geomorphic feature of immense global importance as it exemplifies a unique and fascinating biophysical and ecological process over the entire Indian Peninsula. It influences the weather patterns and is one of the best examples of tropical monsoon system on the planet. The rocks of the Ghats around Mangalore are the charnockites, metamorphic gneisses, granite gneiss etc. with detached occurrences of crystalline limestone, dolerites and anorthosites. Laterisation is extensive and they show two to three different layers with varying texture, physical properties and associations found below the hard, indurated cap. Laterite is characterised by vermicular structure due to the cavities left behind by the dissolving minerals. Just below the hard cap is the softer formations that is subject to problem like landslide and slumping with ground water playing the role of catalyst [1]. The reason for such forms of mass wasting is due to excessive accumulation of water in the pores of formation. The lubricating nature of the interface between permeable beds and impermeable clay within the overburden or the weathered layer can prime gravity movement of slopes leading to land sliding and consequent slumping.

Large scale denudation and dumping of overburden within the refinery campus and years of subsurface erosion due to ground water movement have made the ground prone to failure. Figure-1 shows some of the instances of ground destabilization and failure observed at the site.

Fig. 1. Photographs showing the pattern of ground destabilization at site.

3 Objective of investigation

A comprehensive geophysical investigation was planned using multiple methods to delineate the zone affected by the slope failure at the DHDT site and to characterise the rock mass condition in-situ. It is envisaged that proper restoration and reinforcement works can be initiated based on the findings of the investigation. The specific objectives of the study were as follows:

1. to map the overburden thickness and the profile of hard rock
2. to measure the P & S wave velocities and to derive the shear modulus, Poisson's ratio etc.) of the rock mass
3. to delineate the subsurface weak zones along which the land slide occurred by mapping the lateral/depth extend to the failure surface
4. to map the subsurface drainage pattern and the groundwater flow direction

Four different methods were used to assess the ground condition. Seismic Refraction Survey (SRS), Electrical Resistivity Imaging (ERI), Multichannel Analysis of Surface Waves (MASW) and Cross-borehole Seismic Tomography (CST) were used to derive the different soil/ rock parameters. SRS and MASW were used to estimate the seismic P-wave and S-wave velocity distribution in the subsurface layers (soil/ soft rock/ weathered rock/ destressed rock mass/ hard rock). ERI was carried out to obtain the 2D electrical resistivity distribution in the ground along the line of survey. High-resolution borehole investigation using CST was carried out to map the seismic velocity (p-wave) profile of the ground in the buried portion of the valley where the actual landslide had occurred leading to the damage of piperack.

4 Methodology

4.1 Seismic Refraction Survey

The underlying theory of seismic refraction survey (SRS) is based on the fact that seismic waves (which are essentially elastic mechanical vibrations) travel with different velocities in medium with different densities (rock types). By generating seismic waves at a point and observing the time of arrival of these waves at a number of points on the ground surface, it is possible to determine the seismic velocity distribution in the subsurface. There are two types of seismic body waves, P-wave and S-wave which are widely used in seismic surveys. In a refraction survey, the propagation characteristics of the P-wave is observed and the first arrival time of the P-wave at various geophone locations is used for velocity computations [2].

In the present survey, 10 Hz geophones (24 numbers) were fixed on the ground at 5 m intervals along the line of survey. A 16 lb sledgehammer was used to hit on the shock plate to generate the seismic impulse. Generally, data from 10-12 hammer shots were collected along each survey line and the first arrival times to the geophones were recorded and used for computing the velocity of seismic wave in the subsurface. With a profile length of 115 m, the depth of investigation achieved was about 30-35m.

Computation of velocity from the measured travel time was done by geophysical inversion and hence this technique is also called refraction tomography. The inversion routine involves setting up an initial velocity model by Δt-V method [3] [4] and updating the velocity model iteratively till the RMS error between the calculated travel-time and the measured travel-time is reduced to the minimum. The final velocity model was generated by Wavepath Eikonal Transform (WET) algorithm [5]. The output from the data processing software is plotted by SURFER in terms of contours of seismic velocity at different depths along the profile line. To translate this velocity into the likely geological medium or the rock type, standard tables of seismic velocities is used. However, it is important to note that the seismic velocities overlap for different rocks as they are dependent on several site-specific conditions.

4.2 Electrical Resistivity Imaging

Electrical resistivity imaging is a multi-electrode resistivity surveying technique wherein current is injected into the ground through two current electrodes and potential difference between the potential electrodes on the ground are measured automatically. Owing to the ground heterogeneity and the electrode configuration used, the measured resistivity is the *apparent resistivity* (ρ_{app}). We used dipole-dipole electrode configuration (fig.2) as they are sensitive to lateral as well as vertical variations in ground resistivity. The measurement usually progresses with a spacing of "na" between the current electrodes (C1-C2) and the potential electrodes (P1-P2). The first sequence of measurement is made with a value of n=1 followed by n = 2, 3, 4, 5, 6. As the value of 'n' increases, the measured potential difference becomes smaller and hence the spacing between current electrode is increased and the survey progresses.

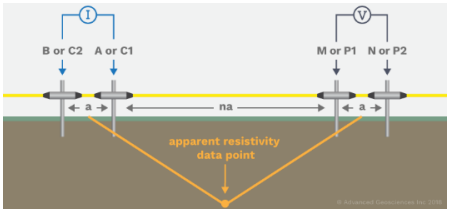

Fig. 2. Dipole-dipole electrode configuration for ERI survey.

In the present ERI survey, 48-electrode system was used with 5 m electrode spacing. The number of recorded data points in each ERI is 1159. The corrected data after removal of bad data is plotted as the apparent resistivity pseudo-section. True resistivity is obtained by inversion (computerised modelling) of the measured apparent resistivity using RES2DINV software [6] [7]. Interpretation of resistivity image in terms of geology is contingent upon knowledge of typical resistivity values for different geological materials. Table-1 shows the range of resistivity and conductivity values for different rocks. It is noted that in-situ values of rock resistivity are sometimes lower due to presence of water and clay minerals.

Table-1. Electrical resistivity & conductivity values for rocks [8].

Material	Resistivity (Ω•m)	Conductivity (Siemen/m)
Igneous and Metamorphic Rocks		
Granite	$5x10^{3}$ - 10^{6}	10^{-6} - $2x10^{-4}$
Basalt	10^{3} - 10^{6}	10^{-6} - 10^{-3}
Slate	$6x10^{2}$ - $4x10^{7}$	$2.5x10^{-8}$ - $1.7x10^{-3}$
Marble	10^{2} - $2.5x10^{8}$	$4x10^{-9}$ - 10^{-2}
Quartzite	10^{2} - $2x10^{8}$	$5x10^{-9}$ - 10^{-2}
Sedimentary Rocks		
Sandstone	8 - $4x10^{3}$	$2.5x10^{-4}$ - 0.125
Shale	20 - $2x10^{3}$	$5x10^{-4}$ - 0.05
Limestone	50 - $4x10^{2}$	$2.5x10^{-3}$ - 0.02
Soils and waters		
Clay	1 - 100	0.01 - 1
Alluvium	10 - 800	$1.25 x10^{-3}$ - 0.1
Groundwater (fresh)	10 - 100	0.01 - 0.1
Sea water	0.2	5

4.3 MASW Survey

MASW technique is one of the seismic exploration methods for determining the shear wave velocity distribution in-situ. It utilises the fact that Rayleigh-type surface waves disperse in a layered medium which in turn can provide key information regarding the rock properties including stiffness coefficient of loose overburden. MASW accurately determines the frequency-dependent phase velocity of fundamental mode of Rayleigh wave, i.e., the shear wave velocity [9]. Layout of MASW survey is shown in figure-3.

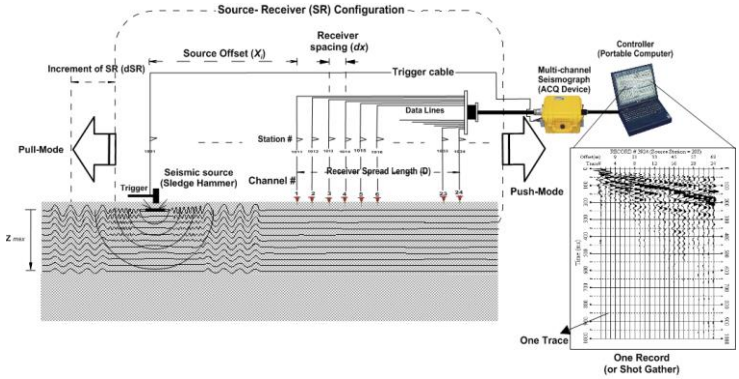

Fig. 3. Schematic diagram showing field set-up of MASW survey

The entire procedure for MASW survey can be explained in three steps: (i) Acquiring multichannel records, (ii) Extracting dispersion curves and (iii) Inverting this dispersion curves to obtain 1D V_s (shear wave velocity) profile. In MASW, several 1D V_s profiles are integrated to obtain the 2D V_s map of the subsurface. In the present investigation, MASW survey was carried out at sites where poor ground condition in the form of landfill sites, heaving ground or areas prone to slope failure was noted. The ration of seismic wave velocities $(\frac{Vp}{Vs})$ and Poisson's ratio (ν) are dependent on lithology, heterogeneity, degree of consolidation, porosity, water saturation, etc. This is mainly because V_p is controlled by the properties like pore/fracture filling material (bulk and shear moduli) for a given density, whereas V_s is controlled by the shear modulus of rock matrix [10]. The Poisson's ratio for isotropic material is given by the equation (1),

$$\nu = \frac{[0.5*\left({}^{Vp}/_{Vs}\right)^2 - 1]}{\left({}^{Vp}/_{Vs}\right)^2 - 1} \qquad \ldots(1)$$

Among the elastic properties, Poisson's ratio is the least studied, but it is one of the most interesting elastic parameters. Poisson's ratio helps in overcoming the non-uniqueness of interpretation when both V_p and V_s fail to infer the actual strata condition. For a well-behaved material, the Young's Modulus and the Poisson's Ratio are two elastic properties that are required to completely define the material's response to applied loads. In case of near surface unconsolidated materials, the $(\frac{Vp}{Vs})$ ratio remains high (>2.0) and hence the Poisson's ratio varies from $\nu \approx 0.32$-0.42. As we go

deeper, the $(\frac{Vp}{Vs})$ ratio reduces (<2.0) and Poisson's ratio decreases to ν≈0.1-0.2 indicating hard and dry rocks [11].

4.4 Crosshole Seismic Tomography

Borehole geophysical method are preferred in area where the surface is not accessible for survey or wherever detailed subsurface mapping is essential for design/stability analysis. Application areas include engineering studies for mapping typical features like fault plane, shear zone, fracture/joint planes, damage assessment, etc., or for precise mapping of seismic velocity [12] [13]. In CST survey measurement of one-way travel time of seismic waves between the source points in one borehole and the receivers in the receiver borehole is made. Usually, electric detonators or borehole sparker is used as seismic source while clamped geophones or hydrophones are used as receivers. During survey, seismic signal from every source point to every receive point is recorded. The raypaths in CST results in an overlapping mesh as shown in figure-4.

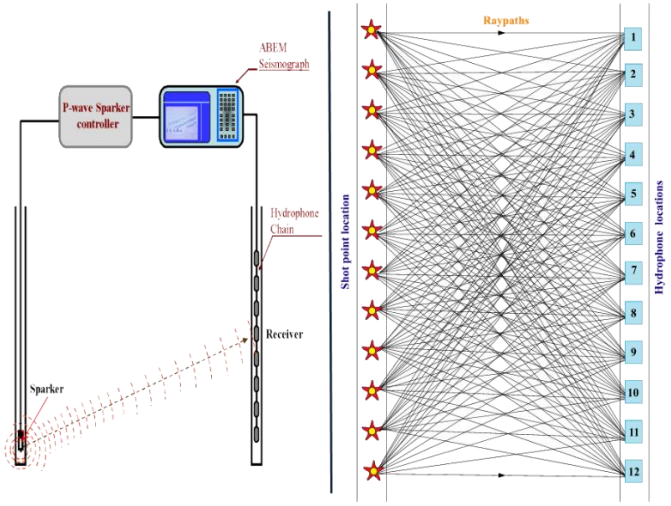

Fig. 4. Schematic layout of CST survey showing raypaths for a 12X12 matrix.

During processing, the time of arrival of seismic signal for each source-receiver pair is determined. For an array of N shot and N receiver positions, we have a matrix of NxN travel-times. The 3D coordinates of every source and receiver positions in the borehole is measured using a deviation probe. The travel-time data & 3D coordinate data are used in tomographic inversion to obtain the seismic velocity distribution between the two boreholes. Data inversion is carried out after dividing the 2D plane separating the boreholes into finite element grid cells and assigning each element in the mesh with a starting velocity. The synthetic travel time data is then iteratively adjusted to converge with the measured travel-time with minimum RMS error [14]. Since there are several raypaths, the process involves simultaneous inversion of all raypaths by an algorithm called Simultaneous Iterative Reconstruction Technique (SIRT) [15]. When the synthetic model converges with the measured values, the RMS

error is the least. At this instance, the model parameters represent the actual velocity distribution in the ground. Velocity tomogram is generated by contouring the seismic velocity at all the grid points. Based on the seismic velocity of the rock mass and the trend of velocity contours, various subsurface layers and anomalous zones are identified and interpreted.

5 Data Acquisition and Processing

In order to map the damage to the foundation area of the piperack due to a land slide spanning about 15-18 m wide, it was necessary to survey the westside of the entire bench where the DHDT/FGTU units are sitting. The entire length of bench was about 345 m and the elevation difference between the bench top and the lower ground was about 8-10 m. Schematic layout of the site plan with survey lines is shown in figure-5.

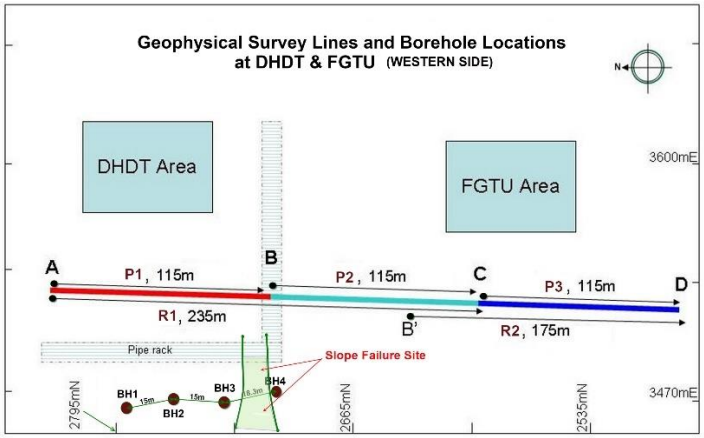

Fig. 5. Layout of the refinery units, damaged zone and geophysical survey lines.

SRS survey was carried out using a 24-channel seismograph (Geode, Geometrics) with geophones (10 Hz) at 5 m interval. Three continuous N-S trending profiles of 115 m each were covered, and they are named **P1**, **P2** and **P3** (Fig-4). Sampling interval was 0.025 ms and the record length was 204 ms. Seismic signal from 8-10 shots were stacked to improve the signal to noise ratio. First breaks were picked up manually and Rayfract software was used for data processing. Seismic velocity sections were presented using Surfer software.

ERI survey was also carried out along the same N-S trending line but with a 48-channel resistivity meter (Syscal R1 Pro) and 5 m electrode interval. Dipole-Dipole electrode configuration was used and data was acquired at 1159 quadrupoles. The profiles were named **R1** and **R2** and their lengths were 235 m and 175 m as shown in figure-5. During data acquisition, stacking was done to improve the data quality and the standard deviation was maintained below 3%. The resistivity data was processed using RES2DINV software and the final output was generated using Surfer software.

MASW survey was carried out along the seismicrefraction profile line P1 and P2, however, we used roll-along setup with 3 m geophone interval. Geode (with 24 channel roll-along), 4.5 Hz geophones, and sledgehammer (16 lbs) was used for the survey. Data was acquired at a sampling interval of 0.25 ms for a record length of 1 s. The MASW profiles were named **M1** and **M2** and they were 141 m in length. Data processing was carried out using SurfSeis Software. Final 2D velocity sections were presented using Surfer software.

CST survey was conducted across three pairs of boreholes. To achieve this, four boreholes were drilled close to the foundation of the piperack covering the damage zone. The separation between the boreholes were 15-18 m and they were drilled up to a depth of 26 m. The tomograms between BH1-BH2, BH2-BH3 and BH3-BH4 were called **Tomo1**, **Tomo2** and **Tomo3** respectively. During data acquisition, the separation between sources and receivers in the respective boreholes was kept at 1 m. Borehole sparker (Geotomographie, GmbH) was used as the source and 12 channel hydrophone chain as receivers. Sampling rate was maintained at 0.025 ms and the record length was 102 ms. State-of-the-art data processing techniques using SIRT routine was used for tomographic inversion. The result was presented using Surfer software.

6 Results and Discussions

Comprehensive geophysical investigations carried out using four different methods have helped in evaluating the damage zone. The results of investigations show that the 2D velocity section from profiles P1, P2 and the 2D resistivity section from profile R1 could delineate the damage zone clearly. These results were very well corroborated by the results from the MASW profiles M1 and M2 and the three tomograms (Tomo1, Tomo2 and Tomo3) from CST survey. Since the results of profile P3 and R2 did not show any adverse ground conditions they are not presented here.

The 2D seismic velocity section derived from SRS along profile P1, P2 and the 2D resistivity section obtained for the same line (profile R1) are shown in figure-6. The shear wave velocity obtained from MASW profiles M1 and M2 along the same survey line (as P1 & P2) is shown in figure-7.

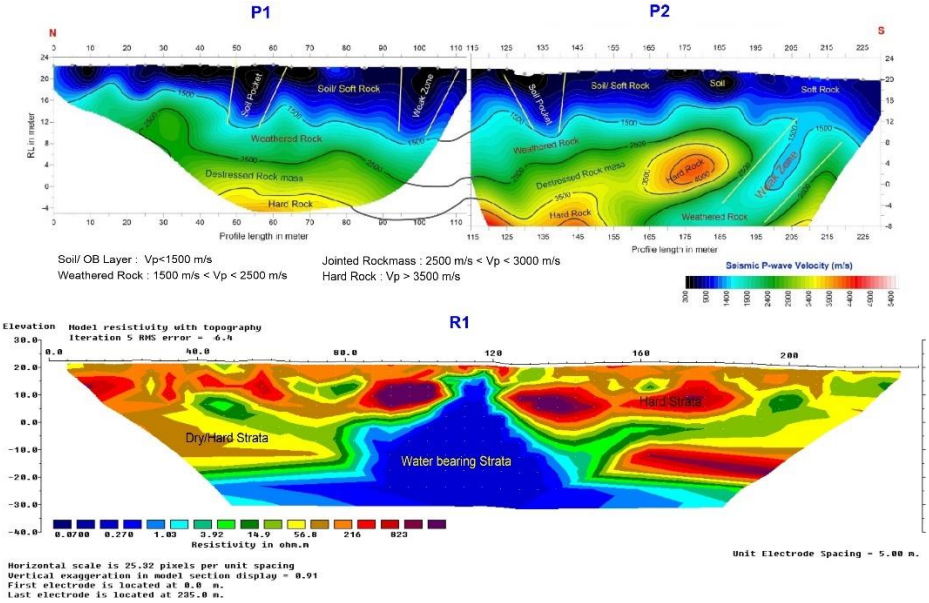

Fig. 6. Seismic velocity sections along P1, P2 and the resistivity section along R1.

The seismic velocity sections are interpreted in terms of overburden (loose soil, soft rock), weathered rock, destressed rock, hard rock and massive rock. The strata classification and the range of velocities attributed to the rock types are given in Table-2.

Table-2. Engineering classification of rock mass based on seismic velocity

Class	Strata Classification	Seismic P-wave velocities	Likely Rock Types/ strata
I	Overburden	< 1500 m/s	Loose & compact soil, soft rock and rock fragments in soil matrix etc.
II	Weathered rock	1500-2500 m/s	Weathered rock/ boulders *or* highly fractured rock mass.
III	Destressed rock mass	2500-3500 m/s	Destressed rock mass with several intersecting joints. They can be strengthened by grouting.
IV	Hard rock	3500-4000 m/s	Hard Rock with in-situ strength in the range of 60-80 MPa.
V	Massive rock	> 4000 m/s	Massive rock with in-situ strength in the range of 80-120 MPa.

Three pockets of loose soil are marked within the overburden where the seismic velocity contours (V_p<800 m/s) show depression. At these locations soft rock seen to extend up to 10 mRL. Weathered rock layer (1500 m/s<V_p<2500 m/s) shows the presence of hard rock boulders and it is also seen in the destressed rock layer. The seismic velocity contour of V_p=2500 m/s marks the beginning of the destressed/jointed rock layer which can be strengthened by consolidation grouting. In profile P1, destressed rock appears at a depth of 10 m in the profile beginning, however, it gets deeper (about 20 m) towards the profile end. In P2, this layer is seen to rise from the profile beginning onwards. The buried valley type feature between 95-

120 m profile distance is prominent. The resistivity section along R1 shows that this buried nallah is water charged completely.

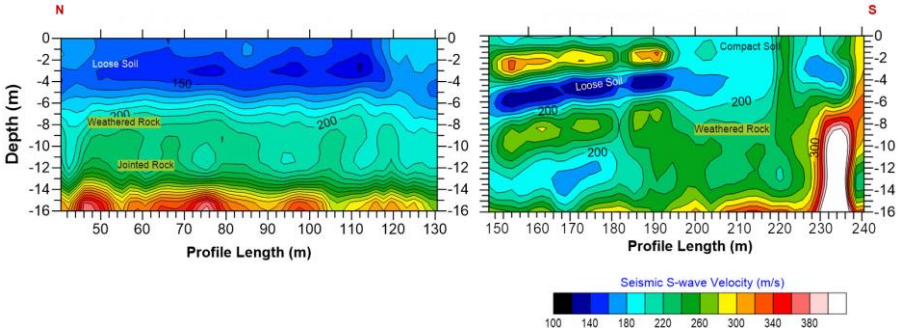

Fig. 7. Shear wave velocity sections along profiles M1 and M2 from MASW survey.

MASW survey shows three layers with prominent shear wave velocity range. They are the loose soil layer (100-180 m/sec) followed by weathered layer (180-280 m/sec) and the destressed rock mass (280-400 m/sec) with depth range of 0-6 m, 6-12 m, and >12 m respectively. Even the shear wave velocity contours show depression at about 100-125 m chainage showing poor rock mass condition. Since the depth of investigation is limited to 16 m, hard rock layer is not clear mapped here. The $(\frac{Vp}{Vs})$ ratio for the profile distance of 0-80 m and 180-240 m shows that it remains between 2-5 indicating better ground condition. However, a study of the 1D graphs of V_p, V_s, $(\frac{Vp}{Vs})$ & Poisson's ratio against depth at 120 m chainage (Fig.8) shows that the $(\frac{Vp}{Vs})$ ratio is 6-8 and the Poisson's ratio of the soil is ν =0.49. The 120 m position is in the middle of the damage zone and the range of $(\frac{Vp}{Vs})$ ratio and Poisson's ratio shows that the ground here is near incompressible where the soil has completely lost its rigidity.

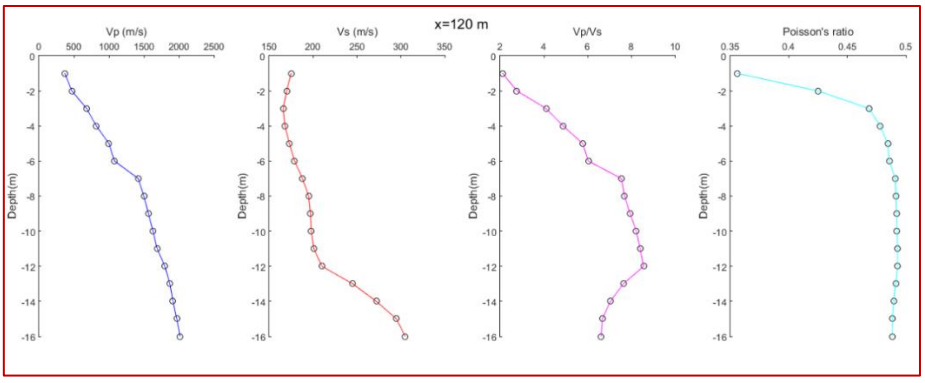

Fig. 8. Graph showing V_p, V_s, $(\frac{Vp}{Vs})$ & Poisson's ratio against depth at X=120 m.

Results of CST survey across the boreholes BH1-BH2, BH2-BH3 and BH3-BH4 are named as Tomo1, Tomo2 and Tomo3. These tomograms are combined together and

are shown in figure-9. The tomograms clearly show the profile of overburden layer and the weathered rock layer. A couple of soil pockets in the overburden layer and in-situ boulders in the weathered and destressed rock layer are clearly mapped.

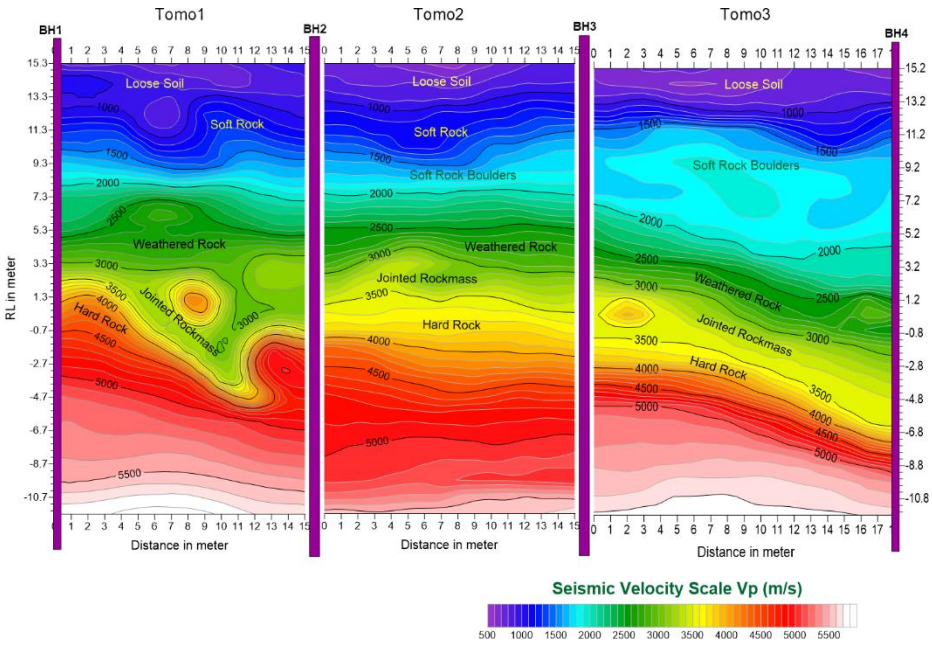

Fig. 9. Results of CST across boreholes BH1-BH2, BH2-BH3 and BH3-BH4.

The profile of hard rock shows that it descends from RL=3 m near BH1 to about RL= -6 m near BH4. This means that continuous hard rock mapped at about 16-17 m in the north of the failure zone has descended to about 21-22 m depth in the valley portion where the slope failure occurred.

7 Conclusions

Geophysical investigations in the refinery Complex for assessment of rock mass condition (qualitative & quantitative) around the damage zone was successful in understanding and characterising the subsurface rock mass conditions to a great extent. The important conclusions drawn from the study are as follows:

1. The profile of the lateritic soil, the weathered rock and the hard rock along the survey lines are clearly delineated.

2. The profile of bed rock showed a valley type feature between 95-120 m chainage and a weak zone showing velocity reversal between chainage 165-210 m extending up to RL= -8 m at the site of piperack foundation.

3. The anomalously low ground resistivity and the $(\frac{Vp}{Vs})$ ratio of 6-8 around the failure zone (95-120 m) showed that the ground is completely saturated. The anomalous-

ly high seismic velocity ratio shows that soil had lost its rigidity after slope failure and following soil piping. This is corroborated by the Poisson's ratio values (ν=0.48-0.49) which defines the ground as near incompressible.

4. In the northern and the southern side of the destabilised zone, the $(\frac{Vp}{Vs})$ ratio of soil is about 3-3.5 implying that the ground is dry and compact. In such areas, the Poisson's ratio of the rock mass is ν =0.40-0.42 which indicates that the ground is compact and rigid.

5. Present study using multiple geophysical methods has helped in integrating the results and in gaining knowledge on ground behaviour that can lead to slope failure. It has helped in accurately mapping the in-situ boulders and the jointed rock/ hard rock interface.

All these information were taken as input for the design of foundations and for planning a comprehensive ground restoration/ reinforcement program including the finalisation of a proper drainage system.

Acknowledgements

This work was carried out on an emergency basis to provide the necessary technical support to a team of engineers carrying out the restoration and reinforcement works. Authors are thankful to all the site engineers and supporting staff from the refinery who worked day and night during the field campaign. Thanks, are also due to the Director, NIRM for giving the necessary permission to take up the investigation work and for providing all the facilities and support.

References

1. Prasad, T.K., Parthasarathy, G.R.: Laterite and Laterisation – A Geomorphological Review. International Journal of Science and Research, Vol. 7, Issue 4, pp. 578-583. (2018).
2. Redpath, B.B.: A seismic refraction exploration for engineering site investigations, Technical Report E-73-4, U.S. Army engineer waterways experiment station, Vicksburg (1973).
3. Gebrande, H., Miller, D.: Refraction Seismic in Angewandte geowissenschaft II, Bender F. (ed). Ferdinand Enke, Stuttgart, pp. 226-260. (1985).
4. Rohdewald, S.R.: Δt-V 1D seismic refraction inversion method interpretation, Rayfract Manual (1999).
5. Schuster, G.T., Quintus-Bosz, A.: Wavepath Eikonal Traveltime Inversion: Theory, Geophysics, V. 58, pp. 1314-1323. (1993).
6. Griffiths, D.H., Barker, R.D.: Two-dimensional resistivity imaging and modeling in areas of complex geology. Journal of applied geophysics, 29, pp. 211-226. (1993).
7. Loke, M.H., Barker, R.D.: Rapid least-squares inversion of apparent resistivity pseudo sections by a quasi-Newton method. Geophysical Prospecting, Vol. 44, pp. 131-152. (1996).
8. Loke, M.H.: Electrical Imaging surveys for environmental and engineering studies: Geoelectrical Course Notes, 136. (2000).
9. Park, C.B., Miller, R.D., Xia, J., Ivanov, J.: Multichannel analysis of surface waves (MASW)-active and passive methods. The Leading Edge, Vol. 26, Issue 1, pp.60-64. (2007).

10. Baglari, D., Dey, A., Taipodia, J.: A state-of-the-art review of passive MASW survey for subsurface profiling, Innovative Infrastructure Solutions, 3, 66, pp. 1-13. (2018).
11. Wang, Q., Ji, S., Sun, S., Marcotte, D.: Correlation between compressional and shear wave velocities and corresponding Poisson's ratios for some common rocks and sulfide ores. Tectonophysics, 469(1-4), pp. 61-72. (2009).
12. Nelliat, S., Jha, P.C., Mohanty, PR.: Imaging of sand lens at a barrage site in the Himalaya-a case study using cross-hole seismic tomography. Journal of the Geological Society of India, 82(5), pp. 529-534. (2013).
13. Butchibabu, B., Sandeep, N., Sivaram, Y.V., Jha, P.C., Khan, P.K.: Bridge pier foundation evaluation using cross-hole seismic tomographic imaging. Journal of Applied Geophysics, 144, pp. 104-114. (2017).
14. Bregman, N.D., Chapman, C.H. Bailey, R.C., Travel time and amplitude analysis in seismic tomography. Journal of Geophysical Research. 94(B6), pp. 7577-7587. (1989).
15. Trampert, J., Leveque, J.J.: Simultaneous iterative reconstruction technique: Physical interpretation based on the generalized least squares solution. Journal of Geophysical Research, 95(B8), pp. 12553-12559. (1990).